IEEE TRANSACTIONS ON
APPLIED SUPERCONDUCTIVITY

A PUBLICATION OF THE IEEE COUNCIL ON SUPERCONDUCTIVITY

JUNE 2017 VOLUME 27 NUMBER 4 ITASE9 (ISSN 1051-8223)

PART II OF THREE PARTS

THE 2016 APPLIED SUPERCONDUCTIVITY CONFERENCE
Denver, CO, USA, September 4–9, 2016

LARGE SCALE

(See first page of Part I for Electronics Table of Contents. Electronics papers begin with Article Number 0100101. See first page of Part II for Large Scale Table of Contents. Large Scale papers begin with Article Number 3500106. See first page of Part III for Materials Table of Contents. Materials papers begin with Article Number 6000105.)

IEEE

IEEE TRANSACTIONS ON APPLIED SUPERCONDUCTIVITY

The IEEE TRANSACTIONS ON APPLIED SUPERCONDUCTIVITY is published by the IEEE Council on Superconductivity, which is sponsored by the IEEE societies listed below. For more information, please visit http://www.ieeecsc.org. Any member of these societies may subscribe to this TRANSACTIONS for $40.00 per year. For information write to the IEEE Service Center at the address below. *Member copies of Transactions/Journals are for personal use only.*

Sponsoring Societies

Communications
H. FREEMAN, *President*
Components, Packaging, and Manufacturing Technology
J. TREWHELLA, *President*
Computer
J.-L. GAUDIOT
Dielectrics and Electrical Insulation
P. LEWIN, *President*
Electron Devices
S. SAHA, *President*
Instrumentation and Measurement
R. DYER, *President*
Magnetics
B. TERRIS, *President*
Microwave Theory and Techniques
K. WU, *President*
Power & Energy
D. NOVOSEL, *President*
Reliability
C. HANSON, *President*
Ultrasonics, Ferroelectrics, and Frequency Control
C. NGUYEN, *President*

Council on Superconductivity

B. STRAUSS, *President*
L. COOLEY, *Vice President-Publications*
A. DELLA CORTE, *Past President*

Editor-in-Chief
B. L. T. PLOURDE
Syracuse University
bplourde@syr.edu

Editors for Materials
P. J. LEE
Florida State University
lee@asc.magnet.fsu.edu

N. NEWMAN
Arizona State University
Nathan.Newman@asu.edu

M. JEWELL
University of Wisconsin Eau Claire
jewellmc@uwec.edu

V. SELVAMANICKAM
University of Houston
selva@uh.edu

Editors for Large-Scale Applications
M. PARIZH
General Electric
parizh@ge.com

S. W. SCHWENTERLY
Oak Ridge National Laboratory (Retired)
schwenterly@ieee.org

P. J. MASSON
University of Houston
pjmasson@uh.edu

A. DEVRED
ITER
Arnaud.Devred@iter.org

L. CHIESA
Tufts University
Luisa.Chiesa@tufts.edu

M. NOE
Karlsruhe Institute of Technology
mathias.noe@kit.edu

S. FARINON
Istituto Nazionale di Fisica Nucleare (INFN)
stefania.farinon@ge.infn.it

C. LUONGO
ITER
Cesar.Luongo@iter.org

A. POLASEK
Electric Power Research Center
polasek@cepel.br

N. AMEMIYA
Kyoto University
amemiya.naoyuki.6a@kyoto-u.ac.jp

Editors for Electronic Applications
A. I. BRAGINSKI
Forschungszentrum Jülich
a.braginski@fz-juelich.de

J. MAZIERSKA
James Cook University
j.mazierska@ieee.org

O. MUKHANOV
Hypres, Inc.
mukhanov@hypres.com

A. W. KLEINSASSER
Jet Propulsion Laboratory
alan.w.kleinsasser@jpl.nasa.gov

D. E. OATES
MIT Lincoln Laboratory
oates@ll.mit.edu

H. ROGALLA
University of Colorado at Boulder
h.rogalla@ieee.org

S. M. ANLAGE
University of Maryland
anlage@umd.edu

C. A. KILBOURNE
NASA Goddard Space Flight Center
Caroline.A.Kilbourne@nasa.gov

IEEE Officers

KAREN BARTLESON, *President*
JAMES A. JEFFERIES, *President-Elect*
WILLIAM P. WALSH, *Secretary*
JOHN W. WALZ, *Treasurer*
BARRY L. SHOOP, *Past President*
S. K. RAMESH, *Vice President, Educational Activities*
SAMIR M. EL-GHAZALY, *Vice President, Publication Services and Products*
MARY ELLEN RANDALL, *Vice President, Member and Geographic Activities*
FORREST D. WRIGHT, *President, Standards Association*
MARINA RUGGIERI, *Vice President, Technical Activities*
KAREN S. PEDERSEN, *President, IEEE-USA*
TOSHIO FUKUDA, *Director, Division X*

IEEE Executive Staff

DR. E. JAMES PRENDERGAST, *Executive Director & Chief Operating Officer*
THOMAS SIEGERT, *Business Administration*
JULIE EVE COZIN, *Corporate Governance*
DONNA HOURICAN, *Corporate Strategy*
JAMIE MOESCH, *Educational Activities*
EILEEN M. LACH, *General Counsel & Chief Compliance Officer*
VACANT, *Human Resources*
CHRIS BRANTLEY, *IEEE-USA*
CHERIF AMIRAT, *Information Technology*
KAREN HAWKINS, *Marketing*
CECELIA JANKOWSKI, *Member and Geographic Activities*
MICHAEL FORSTER, *Publications*
KONSTANTINOS KARACHALIOS, *Standards Association*
MARY WARD-CALLAN, *Technical Activities*

IEEE Periodicals
Transactions/Journals Department

Senior Director, Publishing Operations: FRAN ZAPPULLA
Director, Editorial Services: DAWN MELLEY *Director, Production Services:* PETER M. TUOHY
Associate Director, Editorial Services: WILLIAM A. COLACCHIO *Associate Director, Information Conversion and Editorial Support:* KEVIN LISANKIE
Managing Editor: CHRISTOPHER PERRY *Journals Coordinator:* SHANNON N. CAMPOS

IEEE TRANSACTIONS ON APPLIED SUPERCONDUCTIVITY (ISSN 1051-8223) is published in January, March, April, June, August, September, October, and December by The Institute of Electrical and Electronics Engineers, Inc. Responsibility for the contents rests upon the authors and not upon the IEEE, the Society, or its members. **IEEE Corporate Office:** 3 Park Avenue, 17th Floor, NY 10016-5997. **IEEE Operations Center:** 445 Hoes Lane, Piscataway, NJ 08854-4141. **NJ Telephone:** +1 732 981 0060. **Price/Publication Information:** Individual copies: IEEE members $20.00 (first copy only), nonmember $266.00 per copy. (Note: Postage and handling charge not included.) Member and nonmember subscription prices available on request. **Copyright and Reprint Permissions:** Abstracting is permitted with credit to the source. Libraries are permitted to photocopy for private use of patrons, provided the per-copy fee of $31.00 is paid through the Copyright Clearance Center, 222 Rosewood Drive, Danvers, MA 01923. For all other copying, reprint, or republication permission, write to: Copyrights and Permissions Department, IEEE Publications Administration, 445 Hoes Lane, Piscataway, NJ 08854-4141. Copyright © 2016 by The Institute of Electrical and Electronics Engineers, Inc. All rights reserved. Periodicals Postage Paid at New York, NY, and at additional mailing offices. **Postmaster:** Send address changes to IEEE TRANSACTIONS ON APPLIED SUPERCONDUCTIVITY, IEEE, 445 Hoes Lane, Piscataway, NJ 08854-4141. GST Registration No. 125634188. CPC Sales Agreement #40013087. Return undeliverable Canada addresses to: Pitney Bowes IMEX, P.O. Box 4332, Stanton Rd., Toronto, ON M5W 3J4, Canada. IEEE prohibits discrimination, harassment and bullying. For more information visit http://www.ieee.org/nondiscrimination. Printed in U.S.A.

Digital Object Identifier 10.1109/TASC.2017.2679423

IEEE TRANSACTIONS ON

APPLIED SUPERCONDUCTIVITY

A PUBLICATION OF THE IEEE COUNCIL ON SUPERCONDUCTIVITY

JUNE 2017 VOLUME 27 NUMBER 4 ITASE9 (ISSN 1051-8223)

PART II OF THREE PARTS

THE 2016 APPLIED SUPERCONDUCTIVITY CONFERENCE
Denver, CO, USA, September 4–9, 2016

LARGE SCALE

PAPERS

Superconducting RF

Levitation, Transportation, and Propulsion

(Contents Continued on Next Page)

(Contents Continued from Previous Page)

Magnet Stability, Magentization Effects, AC Losses, and Protection

(Contents Continued on Next Page)

IEEE Transactions on Applied Superconductivity

About this Journal

Aims & Scope

Editorial Board

IEEE Transactions on Applied Superconductivity publication information

Content Announcements

Become a published author in 4 to 6 weeks

Author Resources

IEEE Author Digital Toolbox

Additional Information

IEEE Open Access Publishing Options

Sponsor

Contacts

Editor-in-Chief
Britton L. T. Plourde
Syracuse University
bplourde@syr.edu
http://asfaculty.syr.edu/pages/phy/plourde-britton.html

1.092	0.01158	0.229
Impact Factor	**Eigenfactor**	**Article Influence Score**

Aims & Scope

IEEE Transactions on Applied Superconductivity (TASC) contains articles on the applications of superconductivity and other relevant technology. Electronic applications include analog and digital circuits employing thin films and active devices such as Josephson junctions. Large scale applications include magnets for power applications such as motors and generators, for magnetic resonance, for accelerators, and cable applications such as power transmissions.

Persistent Link: http://ieeexplore.ieee.org/servlet/opac?punumber=77

Frequency: 6

ISSN: 1051-8223

Published by:
- The IEEE Council on Superconductivity

Subjects

Engineered Materials, Dielectrics & Plasmas

Fields, Waves & Electromagnetics

Contacts

Editor-in-Chief
Britton L. T. Plourde
Department of Physics
Syracuse University
223 Physics Building
Syracuse, NY 13244 USA
bplourde@syr.edu
http://asfaculty.syr.edu/pages/phy/plourde-britton.html

Simulation of Screening Current Reduction Effect in REBCO Coils by External AC Magnetic Field

So Noguchi and Vlatko Cingoski

***Abstract*—Second-generation high-temperature superconducting (HTS) tapes have been examined for applications, such as NMR, MRI, and accelerators. Each of these applications requires a precise magnetic field profile. However, screening currents induced while charging an HTS magnet degrade its magnetic field quality. Techniques to reduce the screening current effect have been proposed in the literature. One of the means to reduce screening currents is to apply an AC magnetic field using a "shaking magnet." The shaking effect enhances the quality of magnetic field by reallocating the screening currents inside HTS tapes. Although some experiments to study the shaking field effect were reported, the current distribution inside HTS tapes has not yet been clarified by simulation.**

This paper presents the simulation results for an AC magnetic field applied to a REBCO tape to reduce the influence of screening currents. In addition, we investigated the influence of the angle of applied AC magnetic field at the magnet center. The area of negative current density is also shown. From the simulation results, we conclude that a shaking field applied at an angle between 10 and 30 deg. is effective to reduce the screening current effect.

***Index Terms*—Field homogeneity, REBCO tape, screening current, shaking magnet.**

I. INTRODUCTION

SECOND-generation high-temperature superconducting (HTS) tapes are used to develop ultra-high-field NMR and MRI magnets, e.g., 1.3-GHz NMR [1] and 9.4-T MRI [2]. These HTS applications have two critical problems. The first one is a quench protection, and the other is the field inhomogeneity caused by screening currents. For the former, the No-Insulation winding technique is a promising solution [3], [4]. For the latter, a few techniques to reduce the influence of screening current on the field homogeneity were proposed [5], [6], however, these reports are insufficiently conclusive.

The screening currents deteriorate the field homogeneity in the neighborhood of magnet center [7]. In a REBCO tape, a large screening current is induced by the transverse field due to the tape's flat shape. Recently, the screening current effect on the field homogeneity was clarified by simulation [8]. A promising screening-field reduction solution is to apply a small AC magnetic field to REBCO tapes using a so-called "shaking magnet" [6], [9].

The screening current phenomena in REBCO tapes were investigated in a number of works [8], [10]–[13], in which the simulation models and results were presented. Also, there exist works where the AC field shaking effect on HTS coated conductors was viewed [14], [15]. However, the current distribution caused by the shaking field inside a REBCO tape has not been simulated so far.

In this paper, we employ a 2D finite element method (FEM) just to model the current distribution inside a REBCO tape affected by an external AC magnetic field applied at different angles to the tape wide surface that, in the end, enabled me to find the most effective angle.

II. SIMULATION METHOD AND MODEL

A. Simulation Method

The governing equation is given by

$$\nabla \times \left(\nu \nabla \times \boldsymbol{A}\right) = \boldsymbol{J}_0 + \boldsymbol{J}_\mathrm{S} \tag{1}$$

where ν, $\boldsymbol{A}$, $\boldsymbol{J}_0$, and $\boldsymbol{J}_\mathrm{S}$ are the magnetic reluctivity, the vector potential, the transport current density, and the screening current density, respectively. Here, the transport and screening current densities are defined as follows:

$$\boldsymbol{J}_0 = -\sigma \frac{\partial \boldsymbol{A}'}{\partial t} \tag{2}$$

$$\boldsymbol{J}_\mathrm{S} = -\sigma \left(\frac{\partial \boldsymbol{A}''}{\partial t} + \nabla \phi \right) \tag{3}$$

where $\boldsymbol{A}' + \boldsymbol{A}'' = \boldsymbol{A}$ and ϕ is the scalar potential. Then, $\boldsymbol{J}_0$+$\boldsymbol{J}_\mathrm{S}$ is represented by

$$\int_S \left(\boldsymbol{J}_0 + \boldsymbol{J}_\mathrm{S}\right) \cdot \mathrm{d}\boldsymbol{S} = -\int_S \sigma \left(\frac{\partial \boldsymbol{A}}{\partial t} + \nabla \phi \right) \cdot \mathrm{d}\boldsymbol{S} = I_0 \tag{4}$$

where σ, t, I_0, and $\boldsymbol{S}$ are the electrical conductivity, the time, the transport current, and the cross-sectional area of all the conductors, respectively. In the simulation, we assumed that the current passes only in the z-direction, and that the gradient of ϕ and the electrical conductivity σ are constant within a given finite element. From (4), the following equation is derived [16]:

$$\frac{\partial \phi}{\partial z} = \left(\int_S \sigma \frac{\partial A}{\partial t} \mathrm{d}S - I_0 \right) \Bigg/ \int_S \sigma \mathrm{d}S \tag{5}$$

Substituting (4) and (5) into (1), we obtain the governing equation to be solved using the 2D FEM:

This work was supported in part by the JSPS KAKENHI (Grant Number 15KK0192). Corresponding author: So Noguchi.

S. Noguchi is with the Francis Bitter Magnet Laboratory, Plasma Fusion and Science Center, Massachusetts Institute of Technology, Cambridge, MA 02139, USA as a visiting scientist and with the Graduate School of Information Science and Technology, Sapporo 060-0814, Japan (e-mail: noguchi@ssi.ist.hokudai.ac.jp).

V. Cingoski is with the Faculty of Electrical Engineering, University "Goce Delcev" – Stip, Skopje, 1000, Macedonia.

$$\nu\left(\frac{\partial^2 A}{\partial x^2}+\frac{\partial^2 A}{\partial y^2}\right)=\sigma\left(\frac{\partial A}{\partial t}+\frac{\int_S \sigma\frac{\partial A}{\partial t}\mathrm{d}S-I_0}{\int_S \sigma\mathrm{d}S}\right) \tag{6}$$

Here, the equivalent conductivity of the REBCO layer σ_S is assumed to be derived from the E-J power law:

$$\sigma_S=\frac{|\boldsymbol{J}|}{E_C}\left(\frac{J_C}{|\boldsymbol{J}|}\right)^n \tag{7}$$

where J_C, E_C, n, and $\boldsymbol{J}$ are the critical current, the electric field at the critical current, the index of the power law, and $\boldsymbol{J}_0+\boldsymbol{J}_S$, respectively. The Newton-Raphson method was used to solve the non-linear equations (6), subject to condition (7).

We have developed the 2D FEM program by ourselves. An AC external field is given as a boundary condition. A triangular mesh is employed, and the number of nodes and elements are approximately 2.3 million and 4.7 million, respectively (including 1.6 million nodes and 3.2 million elements for the REBCO layer).

B. Simulation Model

Fig. 1 shows a schematic drawing of the simulation model, ignoring buffer layers in the tape. Table I lists the REBCO tape dimensions and the simulation conditions. The magnetic field components of 6 T and 3 T are applied in the radial and axial directions. Such a combination of the field components is evidenced, for instance, at the end turns of a high-field MRI magnet [2].

In the simulation, a sinusoidal magnetic field, B_{sh}, with an amplitude of 30 mT is applied to the REBCO tape by the shaking magnet (Fig. 2), after the main magnet is fully charged. The shaking field frequency is 50 Hz, and the number of cycles is 3. The shaking field direction relative to the tape (by the field angle) is varied from $\alpha = 0$ to 360 deg. during the simulations. The assumed operating temperature and the transport current were 10 K and 200 A, respectively.

Fig. 3(a) shows the current density distribution in the REBCO layer after the transport current reaches 200 A, where the scale of r axis is enlarged a thousand-fold. The current density nearby the bottom of the REBCO layer is negative due to the screening current effect. The current density distribution shown in Fig. 3(a) represents the initial condition for the shaking field effect simulation.

III. SIMULATION RESULTS

A. Shaking Magnetic Field Parallel to Tape Surface

The simulation was done first with the shaking field applied parallel to the REBCO tape surface, α = 0 deg. The current density distribution for all conductors: copper stabilizer, Hastelloy substrate, silver overlayer, and REBCO layer, at t = 60 ms is shown in Fig. 4. As seen, current flows only in the REBCO layer. Since the current in the REBCO layer cannot be seen in Fig. 4, Fig. 3(b)–(i) show the enlarged current density distributions/maps in the REBCO layer at t = 5, 10, 15, 20, 30, 40, 50, and 60 ms, respectively. At the start of the simulation, the negative current density is observed within a large area, however, the shape of the current-carrying region varies with time. Finally, at 60 ms, large negative currents flow only near the outer surface of the REBCO, while small negative currents flow near the bottom middle of the layer. The shapes of both negative current regions are like thin needles. Such shapes weaken the influence of the screening current on the magnetic field near the magnet center, compared to the initial condition as shown in Fig. 3(a).

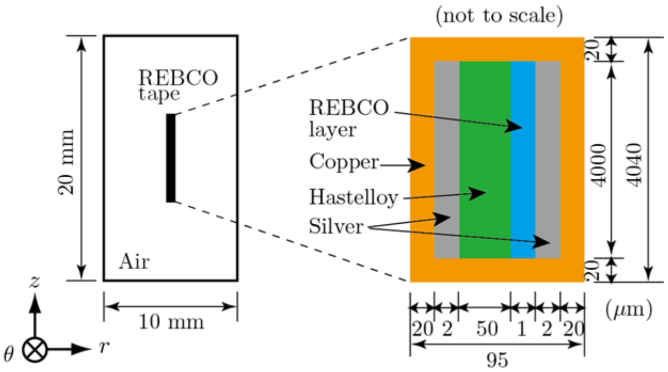

Fig. 1. Schematic drawing of the simulation model (not to scale).

TABLE I
PARAMETERS OF REBCO TAPE AND SHAKING MAGNETIC FIELD CONDITION

REBCO tape	
REBCO tape width	4.04 mm
REBCO tape thickness	0.95 mm
REBCO layer width	4.00 mm
REBCO layer thickness	1 μm
Copper stabilizer thickness	20 μm each side
Silver overlayer thickness	2μm
N-value	20
Magnet condition	
Transport current	200 A
Temperature	10 K
Shaking magnetic field	
Magnitude of shaking field	30 mT (peak)
Shaking field frequency	50 Hz
Number of shaking field cycle	3
Field direction	-30 – 30, 150 – 210 deg.

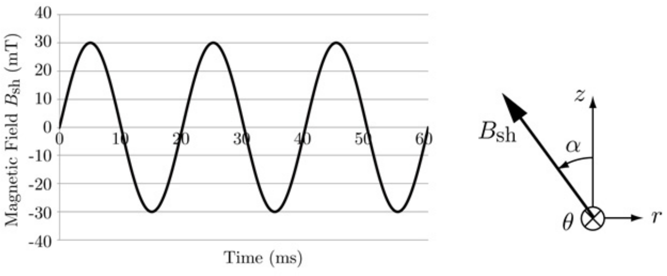

(a) (b)

Fig. 2. External AC magnetic field of 30 mT-peak with angle α (50 Hz, 3 cycles).

B. Various Angled Shaking Magnetic Field

Fig. 5 shows the current density distributions within the REBCO layer at t = 60 ms, when applying the shaking field at the following angles: α = -30 to 30, and 150 to 210 deg.

As seen from Fig. 5, the negative current in the REBCO layer exists far from the coil axis in the cases of α = -30 to 30

This article has been accepted for publication in a future issue of this journal, but has not been fully edited. Content may change prior to final publication. Citation information: DOI 10.1109/TASC.2017.2650864, IEEE Transactions on Applied Superconductivity

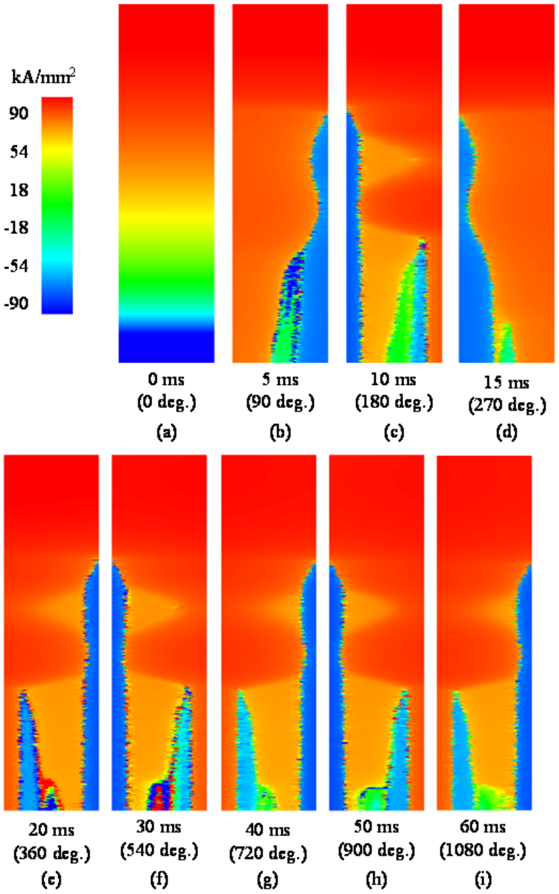

0 ms (0 deg.) (a) 5 ms (90 deg.) (b) 10 ms (180 deg.) (c) 15 ms (270 deg.) (d)

20 ms (360 deg.) (e) 30 ms (540 deg.) (f) 40 ms (720 deg.) (g) 50 ms (900 deg.) (h) 60 ms (1080 deg.) (i)

Fig. 3. Current density distribution of REBCO layer. (a) initial condition, and (b)–(i) the simulation results of $B_{\mathrm{sh}} = 30$ mT and $\alpha = 0$ deg. The r axis is enlarged 1000 times. The numbers in parentheses indicate the phase angle of the magnetic field sweep shown in Fig. 2.

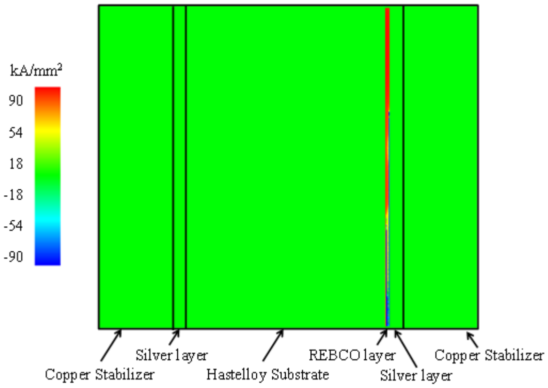

Fig. 4. Current density distribution of REBCO tape. Current does not flow in the copper stabilizer, Hastelloy substrate, or silver overlayers (not to scale).

deg. On the other hand, the negative current is closer to the coil axis when α = 150 to 210 deg. Evidently, the cases of α = -30 to 30 deg. are superior to α = 150 to 210 deg.

IV. EVALUATION OF SHAKING FIELD

It is difficult to quantify the superiority of the shaking field angle on the field homogeneity. In this work, the shaking field is evaluated from the viewpoint of the contribution from a given conductor to the center field and the area of the negative current inside the conductor.

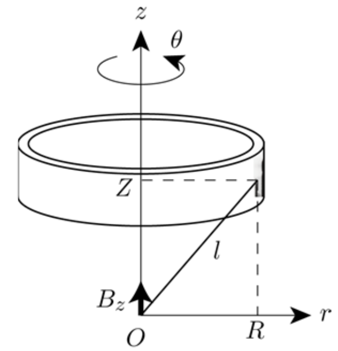

Fig. 6. Schematic drawing of a single-turn coil for evaluation of shaking field effects.

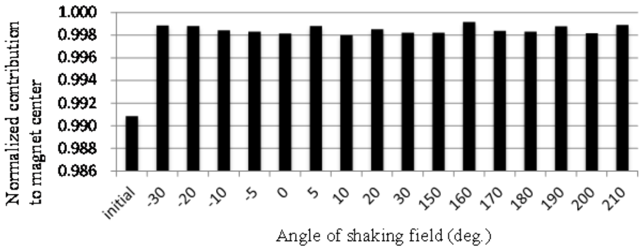

Fig. 7. Normalized contribution of a single-turn coil to the magnet center.

A. Contribution to Center Field

The effect of the current distribution due to the shaking field on the center field is investigated first. In the calculations, the simulated REBCO tape is placed in an arbitrary position. The axial magnetic field generated by a single-turn coil is shown in Fig. 6. The superposition of magnet fields generated by the individual finite elements at the magnet center is given by

$$B_z = \frac{\mu_0}{2}\sum_{i=1}^{n}\frac{J_i S_i r_i^2}{l_i^3} \tag{8}$$

where μ_0, J_i, S_i, r_i, l_i, and n are the permeability of free space, the current density, the area, the radius, and the distance from the origin for ith element, and the total number of finite elements, respectively.

Fig. 7 shows the field contribution at the magnet center for every shaking angle, where the values are normalized to the contribution for an ideal, homogeneous current distribution. The simulated REBCO tape is placed at R = 50 cm and Z = 70 cm. In Fig. 7, the "initial" value means the current distribution just after energizing the single-turn coil. The magnetic field of the initial condition is small, and it approaches 1 after applying a shaking field at any angle to the tape.

Next, Fig. 8 shows the ratio of the field contributions from the negative and positive current B_{z-} / B_{z+}, where B_{z-}, B_{z+} are center field components generated by the negative and positive current, respectively. Since it takes a very long time to decay, it is desirable that the ratio B_{z-} / B_{z+} is close to zero to minimize the screening current effect.

From Fig. 8, the initial condition is the worst among them, *i.e.*, the negative current density appears over a large region close to the magnet center inside the REBCO layer. It would

This article has been accepted for publication in a future issue of this journal, but has not been fully edited. Content may change prior to final publication. Citation information: DOI 10.1109/TASC.2017.2650864, IEEE Transactions on Applied Superconductivity

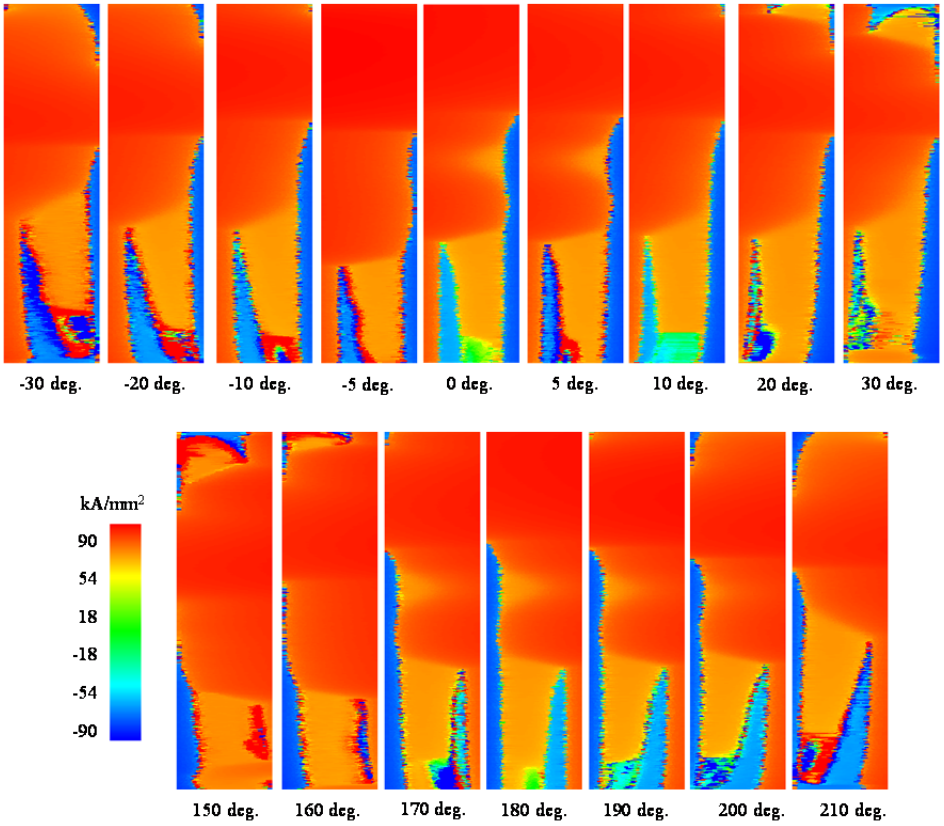

Fig. 5. Current density distribution in REBCO layer at different field angles α = -30–30 and 150–210 deg. at t = 60 ms. The r axis is enlarged 1000 times.

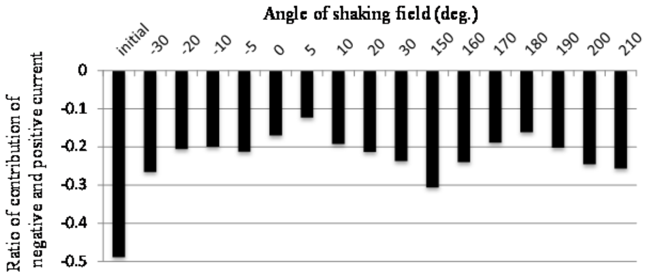

Fig. 8. Ratio of negative and positive contributions to the magnet center.

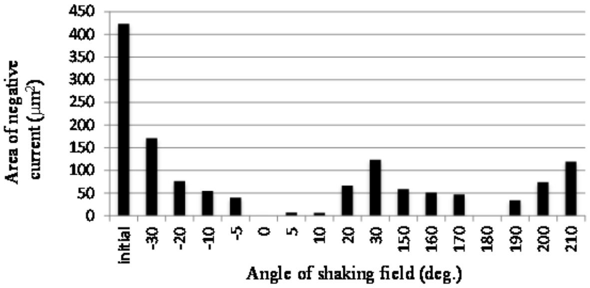

Fig. 9. Area of negative current carrying region.

deteriorate the field homogeneity if the REBCO layer on consideration was in a real magnet winding. From Fig. 8, the angle of 5 deg. minimizes the negative current contribution.

B. Area of Negative Current

Fig. 9 shows the area of the high negative current density (< -60 kA/mm^2) inside the REBCO layer. The area is obviously small at 0–10 and 180 deg.

Considering the above results, the best shaking field angle is between 0 and 10 deg.

V. CONCLUSION

Simulation results of the current distribution inside a REBCO tape in the shaking field applied at different angles are presented. From the obtained simulation results, the center magnetic field generated by a aingle-turn coil with the current distributions is also investigated. The shaking field applied at almost any angle effectively reduces the negative effect of the screening current on the magnet central field. The best shaking field angle value is -30 deg., albeit only from the standpoint of the screening current effect reduction.

Since the negative currents decay for a long time, a minimal amount of negative current is desirable. From the results, we concluded that an AC magnetic field with angle between 0 and 10 deg. produces the greatest shaking effect.

In this paper, only one REBCO tape is considered in the shaking field simulation. However, since there are many turns of a REBCO tape in a magnet, the electromagnetic interaction between the turns should be included appropriately. Also, the authors plan to investigate the effect of the shaking field strength on the screening current reduction.

REFERENCES

[1] J. Bascuñán, S. Hahn, Y. Kim, and Y. Iwasa, “A New High-Temperature Superconducting (HTS) 700-MHz Insert Magnet for a 1.3-GHz

LTS/HTS NMR Magnet," *IEEE Trans Appl. Supercond.*, vol. 23, no. 3, Jun. 2013, Art. ID. 4400304.

[2] T. Tosaka, H. Miyazaki, S. Iwai, Y. Otani, M. Takahashi, K. Tasaki, S. Nomura, T. Kurusu, H. Ueda, S. Noguchi, A. Ishiyama, S. Urayama, and H. Fukuyama, "R&D Project on HTS Magnets for Ultrahigh-Field MRI Systems," *IEEE Trans. Appl. Supercond.*, vol. 26, no. 4, Jun. 2016, Art. ID. 4402505.

[3] S. Hahn, D. K. Park, J. Bascunan, and Y. Iwasa, "HTS Pancake Coils Without Turn-to-Turn Insulation," *IEEE Trans. Appl. Supercond.*, vol. 21, no. 3, pp. 1592-1595, Jun. 2011.

[4] S. Hahn, D. K. Park, J. Voccio, J. Bascunan, and Y. Iwasa, "No-Insulation (NI) HTS Inserts for > 1 GHz LTS/HTS NMR Magnets," *IEEE Trans. Appl. Supercond.*, vol. 22, no. 3, Jun. 2012, Art. ID. 4302405.

[5] Y. Kim, Y. H. Choi, D. G. Yang, H. Shin, M. C. Ahn, H. Lee, "Study for Reducing the Screening Current-Induced Field in a 10-MHz No-Insulation Magnet Using Current Sweep Reversal Method," *IEEE Trans. Appl. Supercond.*, vol. 25, no. 3, Jun. 2015, Art. ID. 4601005.

[6] K. Kajikawa and Y. Okabe, "Reduction of Screening-Current-Induced Fields in an HTS Tape Winding Using Toroidal Arrangement of Shaking Coil," *IEEE Trans. Appl. Supercond.*, vol. 26, no. 4, Jun. 2016, Art. ID. 4400504.

[7] M. C. Ahn, T. Yagai, S. Hahn, R. Ando, J. Bascunan, and Y. Iwasa, "Spatial and Temporal Variations of a Screening Current Induced Magnetic Field in a Double-Pancake HTS Insert of an LTS/HTS NMR Magnet," *IEEE Trans. Appl. Supercond.*, vol. 19, no. 3, pp. 2269-2272, Jun. 2009.

[8] H. Ueda, Y. Imaichi, T. Wang, A. Ishiyama, S. Noguchi, S. Iwai, H. Miyazaki, T. Tosaka, S. Nomura, T. Kurusu, S. Urayama, and H. Fukuyama, "Numerical Simulation on Magnetic Field Generated by Screening Current in 10-T-Class REBCO Coil," *IEEE Trans. Appl. Supercond.*, vol. 26, no. 4, Jun. 2016, Art. ID. 4701205.

[9] K. Kajikawa, G. V. Gettliffe, Y. Chu, D. Miyagi, T. P. Lécrevisse, S. Hahn, J. Bascuñán, and Y. Iwasa, "Designs and Tests of Shaking Coils to Reduce Screening Currents Induced in HTS Insert Coils for NMR Magnet," *IEEE Trans. Appl. Supercond.*, vol. 25, no. 3, Jun. 2015, Art. ID. 4300305.

[10] J. Xia, H. Bai, J. Lu, A. Gavrilin, Y. Zhou, and H. Weijers, "Electromagnetic modeling of REBCO high field coils by the H-formulation," *Supercond. Sci. Technol.*, vol. 28, no. 12, Oct. 2015 Art. ID. 125004.

[11] N. Amemiya, Y. Sogabe, M. Sakashita, Y. Iwata, K. Noda, T. Ogitsu, Y. Ishii, and T. Kurusu, "Magnetisation and field quality of a cosine-theta dipole magnet wound with coated conductors for rotating gantry for hadron cancer therapy," *Supercond. Sci. Technol.*, vol. 29, no. 2, Dec. 2015, Art. ID. 024006.

[12] L. Quéval, V. Zermeño, and F. Grilli, "Numerical models for ac loss calculation in large-scale applications of HTS coated conductors," *Supercond. Sci. Technol.*, vol. 29, no. 2, Jan. 2016, Art. ID. 024007.

[13] E. Pardo, "Modeling of screening currents in coated conductor magnets containing up to 40000 turns," *Supercond. Sci. Technol.*, vol. 29, no. 8, Jun. 2016, Art. ID. 085004.

[14] V. Lahtinen, E. Pardo, J. Šouc, M. Solovyov, and A. Stenvall, "Ripple field losses in direct current biased superconductors: Simulations and comparison measurements," *J. Appl. Phys.*, vol. 115, 2014, Art. ID. 113907.

[15] Z. Xu and F. Grilli, "Modelling ac ripple currents in HTS coated conductors," *Supercond. Sci. Technol.*, vol. 28, no. 10, Aug. 2015, Art. ID. 104002.

[16] T. Nakata, N. Takahashi, and K. Fujiwara, "Physical meaning of gradϕ in eddy current analysis using magnetic vector potentials," *IEEE Trans. Magn.*, vol. 24, no. 1, pp. 178-181, Jan. 1988.